

THE VELOCITY FIELD PRODUCED BY A SUBMERGED JET DIRECTED UPWARDS AT A FREE SURFACE

A. D. GARRAD

Wind Energy Group, Taylor Woodrow Construction, 309 Ruislip Road East, Greenford, Middlesex, UB6 9BQ, U.K.

and

M. A. PATRICK

Department of Chemical Engineering, University of Exeter, Exeter, Devon, U.K.

(Received 14 September 1982 and in final form 25 November 1982)

Abstract—This paper considers the flow in a round, turbulent submerged water jet directed normally at a free water surface from below. Axial velocity distributions are presented and compared to those of the corresponding free jet. The radial velocity distribution on the surface above the jet was measured and these results are presented and compared with the distribution for a wall jet produced by jet impingement on to a rigid surface. The overall pattern of the flow in the test tank was observed by flow visualisation. It is demonstrated that knowledge of these parameters will be useful in modelling heat and mass transfer in flows of this kind.

NOMENCLATURE

- a , location of apparent jet origin;
- A , numerical constant;
- d , diameter of jet at nozzle exit;
- h , depth measured vertically downwards from the free surface;
- H , height of free surface above nozzle exit;
- r , radial distance measured from jet axis;
- $r_{1/2}$, value of r at which u_z has fallen to half of its axial value;
- Re_j , jet exit Reynolds number, $U_0 d / \nu$;
- u_r , radial velocity;
- u_z , axial velocity;
- U_0 , jet exit velocity;
- z , vertical distance above nozzle.

Greek symbols

- ν , kinematic viscosity of water.

1. INTRODUCTION

IN WATER purification, waste-water disposal, industrial mixing plant and water circulation systems, situations can arise in which a turbulent jet is directed upwards at a free surface. In such processes it is important to have information about the resulting flow pattern and likely mass transfer behaviour, relating for example to oxygen absorption at the surface.

The present work considers the nature of the flow produced when a circular water jet is directed upwards at a free surface. Laser anemometry and flow visualisation were used to measure both the axial velocity distribution and the velocity profile of the radial flow beneath and parallel to the free surface. Flow visualisation was also used to establish the nature of the flow pattern in the tank as a whole.

Surprisingly little information seems to be available on flows of this kind. Free jets are adequately treated in

standard texts [1, 2]; jets impinging on solid surfaces are also fairly well documented [3, 4]. Davies [5] mentions unpublished work by Davies and Orridge [6] on the behaviour of jets impinging on free surfaces and some further work on the turbulence characteristics of these jets is described by Davies and Lozano [7]. Banks and Bhavamai [8] report some analytical and experimental studies on jets impinging on heavier liquid.

2. EXPERIMENTAL APPARATUS

A closed-circuit system (Fig. 1) was used in which water was pumped from an outlet of large diameter into the test tank, via a rotameter and control valve, and returned through an ASME long radius profile nozzle with an exit diameter of 5.98 mm and a diameter ratio of 2. The jet issued from this nozzle had an essentially flat velocity profile. The tank was square in cross-section with side 36.8 cm. It was constructed mainly of Perspex but was fitted with two sides of high-quality glass through which optical measurements were made.

Point velocity measurements in the tank were made using a laser anemometer operating in the reference-beam mode (Fig. 2). The system was modelled on that used by Denham and Patrick [9]. The single laser beam

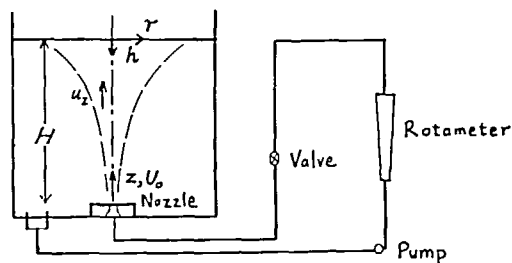


FIG. 1. The flow system used for the experiment.

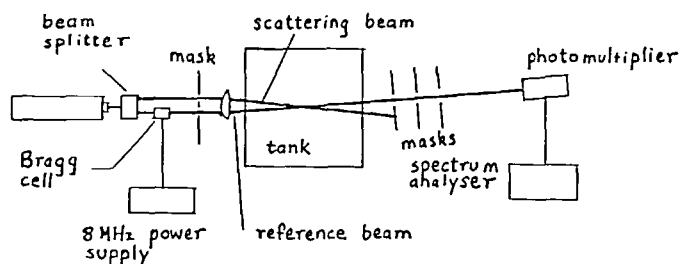


FIG. 2. The laser Doppler anemometer.

was divided using a beam splitter and the 'reference' beam passed through a Bragg cell driven at a frequency of 8 MHz by a crystal-controlled oscillator. One of the resulting first-order frequency-shifted beams, together with the 'scattering' beam, were focused onto the point of interest in the flow system. Light scattered from particles within the measurement point was then heterodyned at the photomultiplier with light from the reference beam. Careful masking was employed to reduce the amount of stray light incident on the photocathode. The photomultiplier output was processed using a spectrum analyser which yielded information enabling the mean velocity at the measuring point to be calculated.

Some further velocity measurements were made using a simple glass pitot tube suspended directly above the nozzle. The dynamic head was measured directly as the height of the column of water in the tube above the mean level in the tank.

Flow visualisation was also employed. The water was seeded with small, neutrally buoyant, spherical polystyrene particles. A powerful light source

illuminated a plane in the tank containing the nozzle. Long exposure photographs taken of this plane revealed the flow pattern.

3. RESULTS AND DISCUSSION

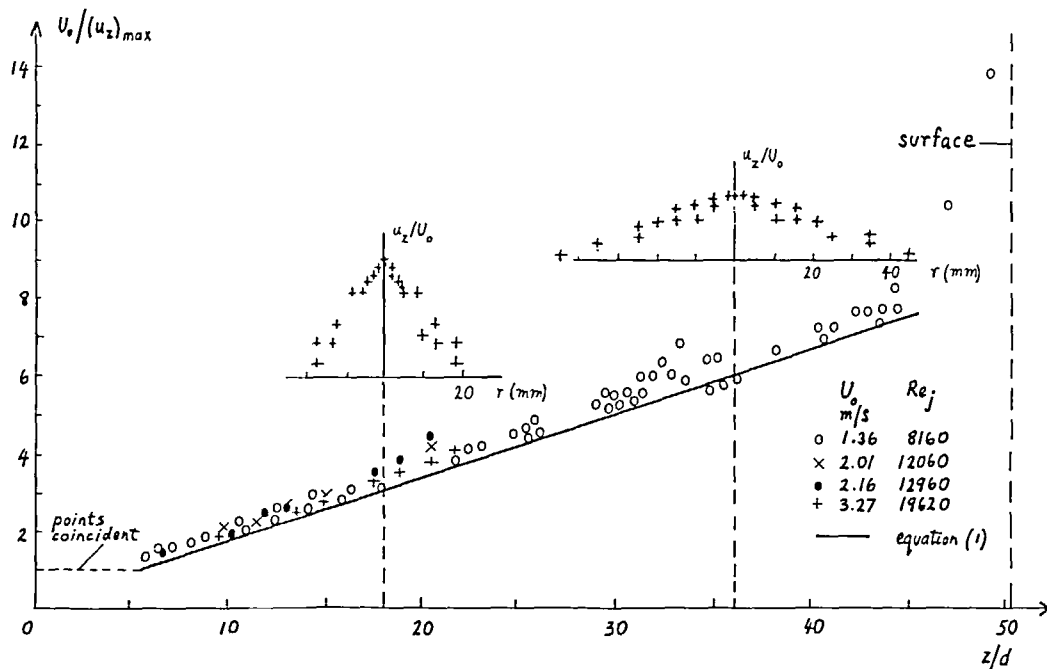
3.1. Vertical velocity measurements

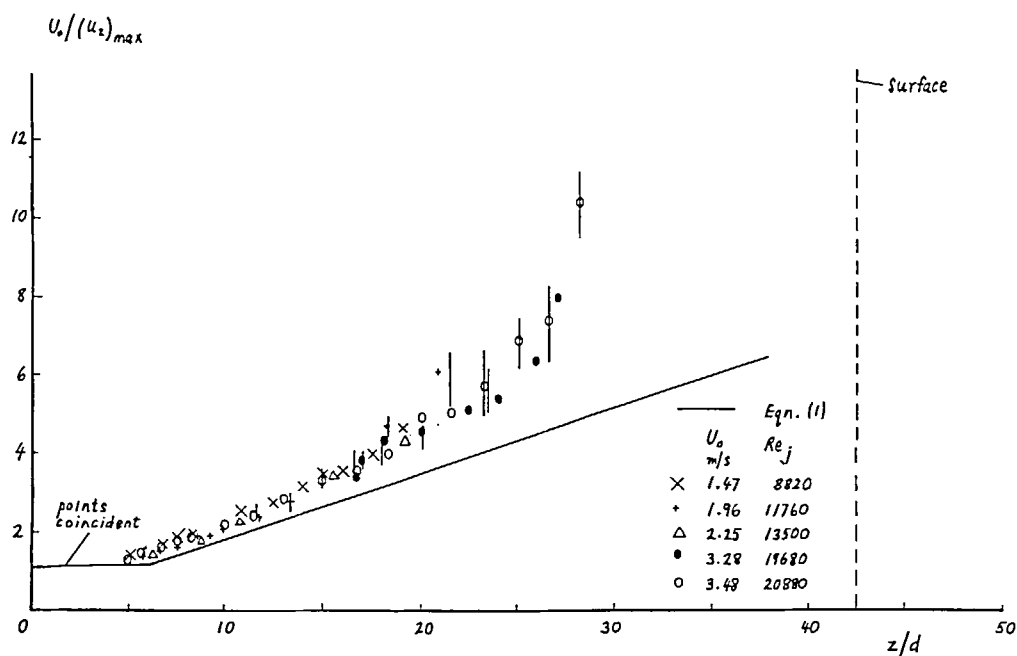
The notation used is shown in Fig. 1. Velocity measurements were made along the jet axis, at various nozzle exit speeds for three values of liquid depth, $H = 30.5, 25.5$ and 17.5 cm. The results are shown in Figs. 3–5 plotted in non-dimensional form as $U_0/(u_z)_{\max}$ vs z/d , where d is the jet diameter at exit. On each graph a theoretical line is also drawn representing the velocity decay of the corresponding free jet, which according to Hinze [2] is given by

$$\frac{(u_z)_{\max}}{U_0} = A \frac{d}{z+a}. \quad (1)$$

Different authors use different values for A and a . Here $A = 5.9$ and $a = -0.5d$.

Each distribution has a constant-velocity region

FIG. 3. Vertical velocity distribution, $H = 30.5$ cm.

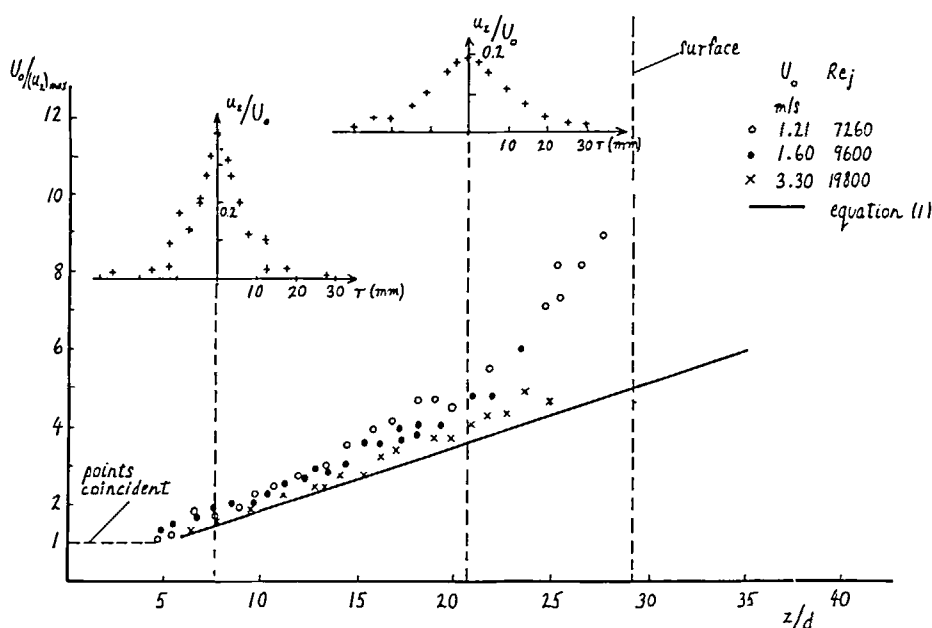
FIG. 4. Vertical velocity distribution, $H = 25.5$ cm.

near the jet exit which can be assumed to be inside a 'potential' core. This is followed by a self-preserving region in which the jet velocity is approximately inversely proportional to z . As the surface is approached the velocity rapidly tends to zero.

The velocity distribution for the largest value of H , shown in Fig. 3, follows the decay curve for a free jet most closely. The experimental points form a line that runs parallel to the theoretical one with the same

gradient but a different origin. The theoretical origin depends on the choice of a . Some authors have used values as large as $a = -3d$, so the proper choice of the virtual origin seems to be a matter of some debate, and probably depends on the detailed mean velocity and turbulence profiles at the nozzle exit.

For $H = 25.5$ cm (Fig. 4) the measurements were made using a simple pitot tube. The unreliability of this method for measurement of low velocities accounts for

FIG. 5. Vertical velocity distribution, $H = 17.5$ cm.

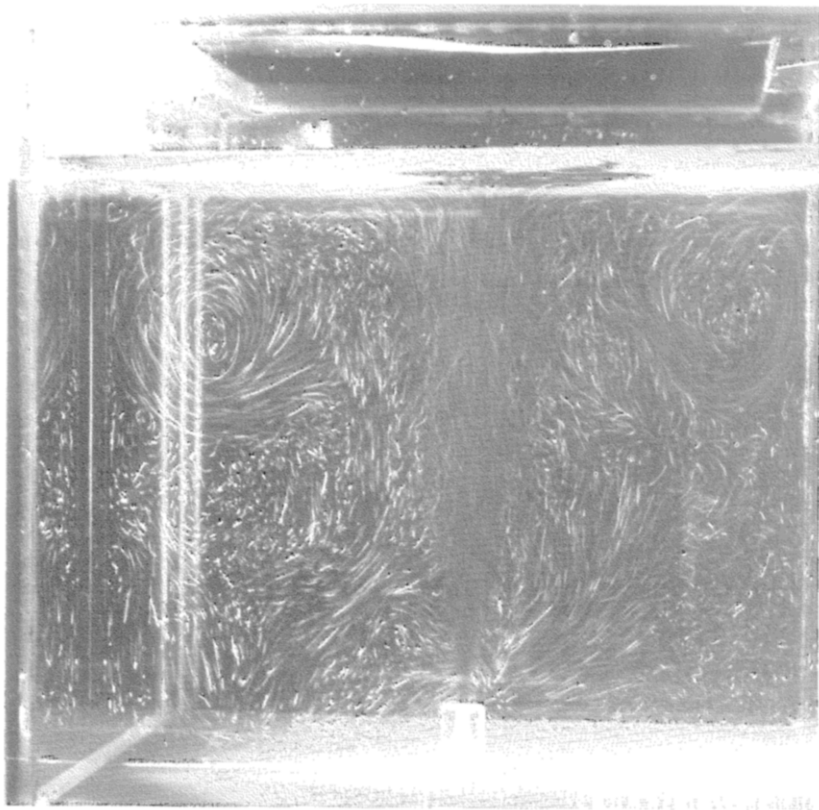


FIG. 6. Flow patterns, $H = 30.5$ cm.

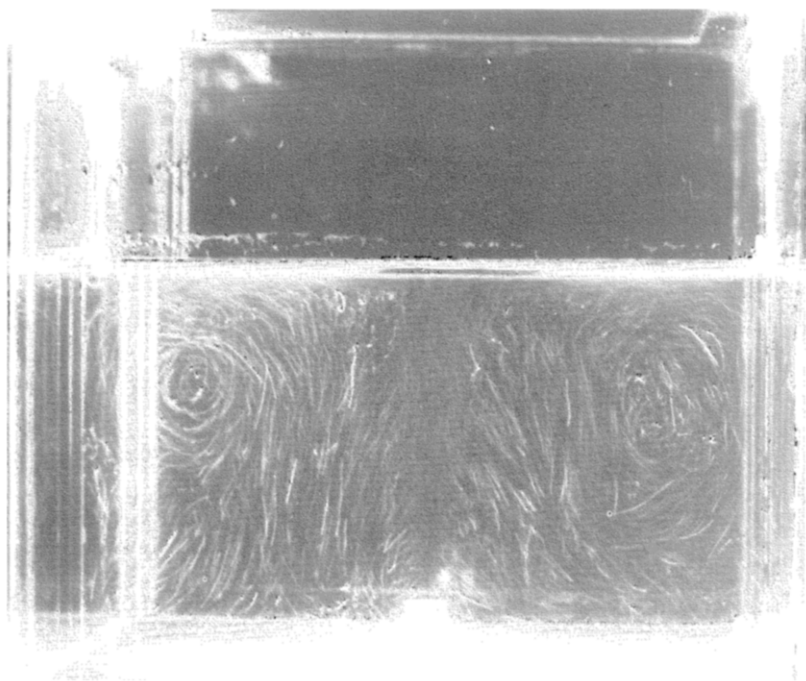


FIG. 7. Flow patterns, $H = 17.5$ cm.

the large uncertainty of the data points and the absence of any readings near the surface.

Figure 5 shows the velocity decay for the smallest value of H , 17.5 cm. This shows qualitatively the same behaviour as the other two depths, but is particularly interesting since it also exhibits a slight Reynolds number dependence. In each of Figs. 3–5 both the jet exit velocity U_0 [m s^{-1}] and the jet exit Reynolds number $Re_j (= U_0 d/\nu)$ are indicated. In Fig. 5 it will be noted that as Re_j increases the distribution departs from the linear relation at an earlier stage. A similar Reynolds number effect has been observed for jets impinging on a rigid surface [3]. However, the major factor determining the height at which the experimental points diverge from the linear curve is the proximity of the surface rather than the jet exit Reynolds number.

For $H = 30.5$ and 17.5 cm a radial traverse was made at two heights producing the two distributions of axial velocities plotted in Figs. 3 and 5. Each pair shows how the jet broadens with height. At the nozzle exit it is 6 mm in diameter.

The photographs in Figs. 6 and 7 show that the jet axis is not precisely vertical. Jets are commonly observed to 'flap' from side to side, such behaviour was reported by Donaldson and Snedeker [3]. The velocity measurements shown in Figs. 3–5 were made along a line vertically above the nozzle exit. The fact that the jet axis is not coincident with this line helps to explain the discrepancy between the predicted and measured values in these figures since off-axis measurements will tend to reduce the magnitude of the velocity.

The flow visualisation photographs show quite clearly the overall flow patterns that are established. The main features are the fast moving vertical jet that broadens to form symmetrical radial flow near the surface, and gives rise to a toroidal circulation eddy adjacent to the tank walls.

The jet is not, of course, discharging into an infinite medium as is assumed in the derivation of equation (1) so that the axial velocity decay is rather more rapid than for a free jet.

Expressions exist for the rate at which a free jet

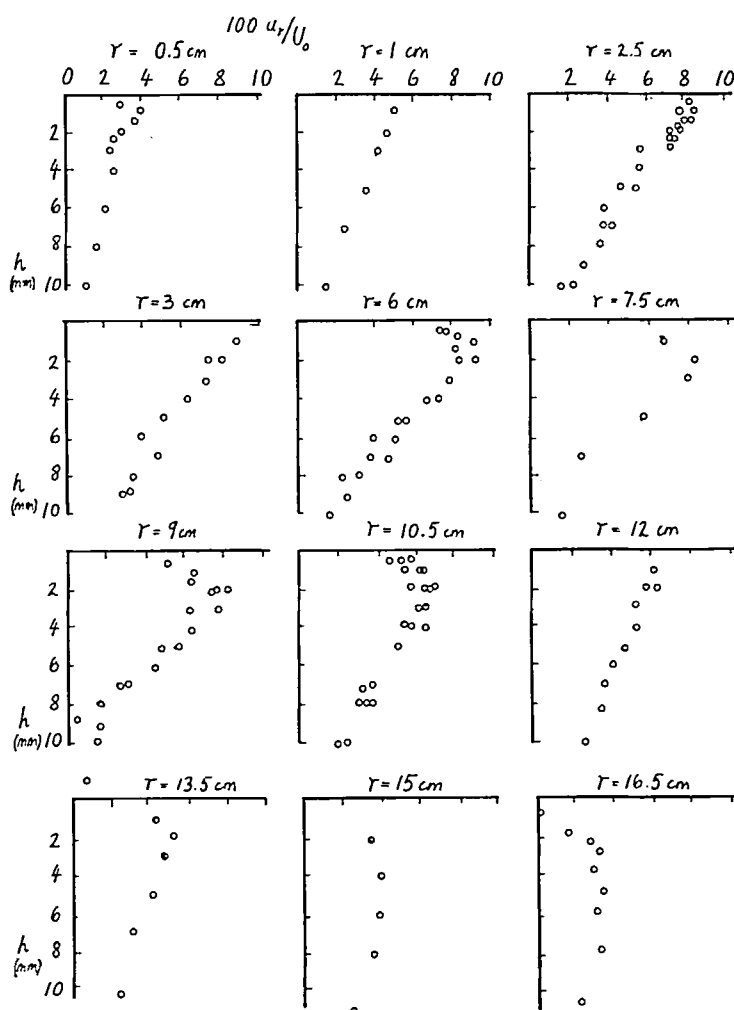
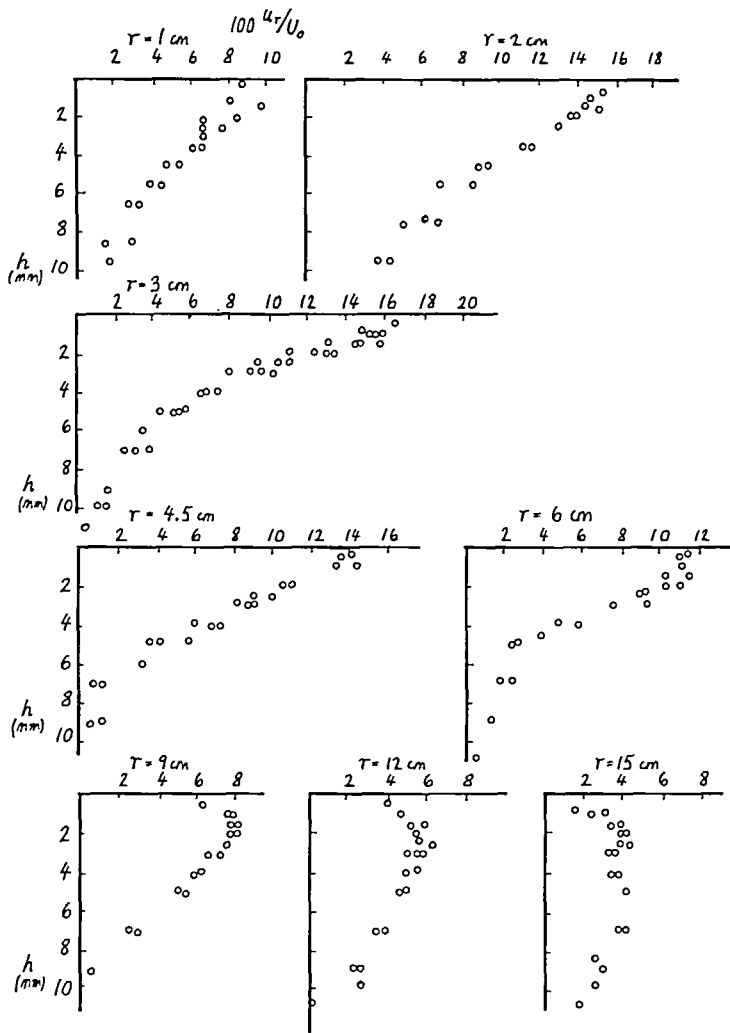


FIG. 8. Radial velocity distribution beneath the free surface, $H = 30.5$ cm.

FIG. 9. Radial velocity distribution beneath the free surface, $H = 17.5$ cm.

broadens with axial distance. Hinze [2] gives

$$r_{1/2} = 0.08(z + a)$$

and Schlichting [1] (2)

$$r_{1/2} = 0.0848(z + a)$$

where $r_{1/2}$ is the radius at which the axial velocity has fallen to half the maximum value at the same height.

For $H = 30.5$ and 17.5 cm, profiles of u_z vs r were measured. These measurements allow approximate values for $dr_{1/2}/dz$ to be calculated. For $H = 17.5$ cm $dr_{1/2}/dz = 0.08$ and for $H = 30.5$ cm it is 0.14 . By differentiating equations (2) with respect to z

$$\frac{dr_{1/2}}{dz} = 0.08 \text{ to } 0.085. \quad (3)$$

It should be mentioned that for $H = 17.5$ cm the radial traverses were made for $U_0 = 1.21 \text{ m s}^{-1}$ whereas for $H = 30.5$ cm the value of 1.36 m s^{-1} was used.

At the free surface the jet has effectively broadened to fill the width of the tank, and is therefore much broader

than would be expected for a free jet at the same distance from the nozzle. In the light of this it is easy to explain the large increase in the broadening rate that was observed for $H = 30.5$ cm. For the smaller value of H the broadening rate is the same as that for a free jet, probably because the measurements were made in a region where the effect of the free surface and containing walls was not yet felt.

3.2. Radial velocity distribution near the surface

The radial velocity profiles are shown in Figs. 8 and 9. The velocities are made non-dimensional with respect to U_0 and the depth h is in mm. The flow forms a thin shear layer near the surface. Near the jet axis the radial velocity increases quite sharply towards the interface. Davies and Lozano [7] report similar behaviour for the water-air interface that they investigated. Unfortunately they only give quantitative results for the turbulence intensity distribution and so it is not possible to make a detailed comparison. As r increases the profiles undergo a change in shape. Near the jet axis

the velocity appears to be approximately linearly dependent on h . As r increases a point of inflexion appears, so that the maximum velocity no longer occurs at the surface but slightly below it. In the proximity of the wall, extrapolation of the profiles indicates that there may in fact be negative velocities near the surface.

The flow visualisation photographs provide a possible explanation for this change in shape of the profile. Small particles were used to seed the flow before the photographs were taken. They are neutrally buoyant in water but nevertheless many found their way to the surface. Figures 6 and 7 show them clearly lying on it. They surround a patch directly above the jet which has been swept clean by the continual action of the jet.

It can probably be assumed that the shear stress applied to the water surface by the air is negligible. Potential flow with a free upper surface that is contained by vertical walls will exhibit profiles similar to those shown in Figs. 8 and 9. There is however an additional retarding force which results from the presence of the dirt particles and any other solid matter that may be lying on the surface. It has been reported [10] that in order to obtain a truly free surface the experiment must be conducted in a vacuum and the water be distilled at least twice. The shape of the surface profiles is sensitive to the presence of surface pollutants.

If the free surface were replaced by a wall, the jet formed along its surface would be known as a wall jet, by analogy the jet formed at the surface will be known as a "free-surface" jet. It is thought that due to the relative proximity of the sides of the tank to the jet axis, the free-surface jet never becomes fully formed. The influence of the tank sides is felt before the influence of the axial jet at the centre of the tank has become unimportant.

Very near the sides of the tank surface tension and wall effects are felt. The presence of small surface waves was observed in this region.

It was not possible to measure the velocity actually at the surface because the meniscus at the walls precluded use of the laser anemometer.

In order to estimate it the profiles of Figs. 8 and 9 were extrapolated to the surface. These estimates of surface velocity are shown in Fig. 10. On the jet axis and on the side walls the velocity is zero, so the surface velocity reaches a maximum value between these two points.

The detailed study of Banks and Bhavamai [8] which explored the behaviour of a liquid jet impinging normally on a heavier immiscible liquid might have afforded some comparison with the present work. Their investigation was centred about the cavity produced in the impingement surface; the equivalent protruberance created by the water jet in the present study was not the subject of any quantitative experiments and so meaningful comparisons are not possible.

3.3. Mass transfer at the surface

For jets impinging on a rigid surface it can be shown [3, 4] that the heat transfer rate (and, therefore, by analogy the mass-transfer rate) at the stagnation point depends strongly on the value of du_r/dr there. This quantity could easily be evaluated from Fig. 10, but its relevance to mass transfer in the case of a free surface is not clear. No similar dependence is known for such jets.

Davies [5] quotes results from Orridge [6] on the mass transfer in just the situation considered here. These results indicated that the maximum mass-transfer rate occurs when the jet nozzle is approximately 28 nozzle diameters from the surface as compared with 8 diameters for a jet impinging on a rigid surface. The mechanism involved must therefore be very different in the two cases.

The surface-renewal rate is the essential mechanism for mass transfer. The Higbie and Danckwerts models

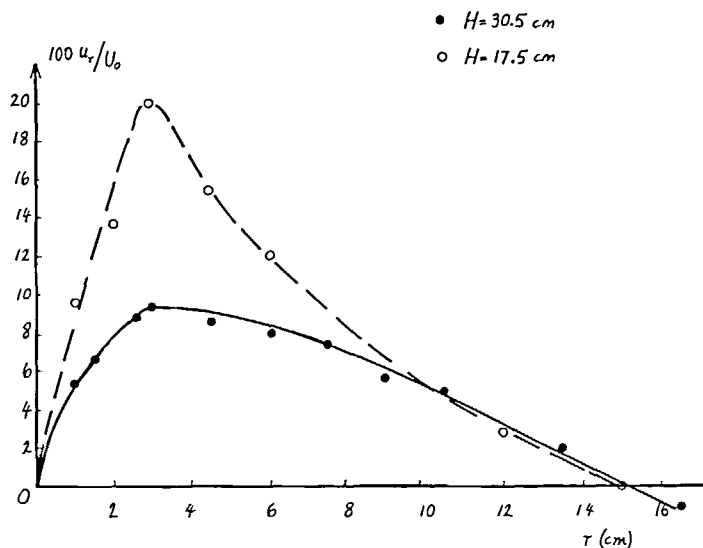


FIG. 10. Distribution of radial velocity at the free surface.

both require some information about the behaviour of the turbulent eddies near the surface in order to estimate the transfer rate that occurs there. A value for the surface-renewal rate or the contact time could perhaps be derived from knowledge of the radial velocity at and near the free surface. The more sophisticated "roll-cell" or Fortescue-Pearson model [11] needs information about the turbulence intensity and the turbulent mixing length. To make a realistic estimate of the latter the surface velocity profiles would be useful.

Mass-transfer rates are usually calculated by superimposing some turbulence model on the mean flow profiles which may be calculated, guessed or modelled on experimental data. Whatever approach is used the surface velocity profiles must play an important role in the understanding and prediction of the mass transfer at a free surface.

4. CONCLUSIONS

The axial velocity decay for a jet impinging on a free surface is initially similar to that for a free jet, however, velocity decays rapidly as the free surface is approached.

The radial surface-velocity profiles are interesting in that they exhibit a change in shape as the distance from the jet axis increases.

It is thought that the details of the flow near the surface should prove useful for studies of heat and mass transfer in liquid systems stirred by submerged jets.

REFERENCES

1. H. Schlichting, *Boundary-Layer Theory* (6th edn.) p. 699. McGraw-Hill (1968).
2. J. O. Hinze, *Turbulence* (2nd edn.), p. 538. McGraw-Hill (1975).
3. C. D. Donaldson and R. S. Snedeker, A study of free jet impingement, Part I, *J. Fluid Mech.* **45**, 281-319 (1971).
4. C. D. Donaldson, R. S. Snedeker and D. P. Margolis, A study of free jet impingement, Part II, *J. Fluid Mech.* **45**, 477-512 (1971).
5. J. T. Davies, *Turbulence Phenomena*. Academic Press (1972).
6. M. A. Orridge, Ph.D. Thesis, Chem. Eng. Department, University of Birmingham, U.K. (1970).
7. J. T. Davies and F. J. Lozano, Turbulence characteristics and mass transfer at air-water surfaces, *A.I.Ch.E. J.* **25**, 405-415 (1979).
8. R. B. Banks and A. Bhavamai, Experimental study of the impingement of a liquid jet on the surface of a heavier liquid, *J. Fluid Mech.* **23**, 229-240 (1965).
9. M. K. Denham and M. A. Patrick, Laminar flow over a downstream facing step in a two-dimensional flow channel, *Trans. Instn Chem. Engrs* **52**, 361-367 (1974).
10. N. Thomas, Department of Applied Mathematics and Theoretical Physics, University of Cambridge, private communication.
11. G. E. Fortescue and J. R. A. Pearson, On gas absorption into a turbulent liquid, *Chem. Engng Sci.* **22**, 1163-1176 (1967).

CHAMP DE VITESSE PRODUIT PAR UN JET SUBMERGÉ DIRIGÉ VERS LE HAUT SUR UNE SURFACE LIBRE

Résumé—On considère l'écoulement relatif à un jet d'eau submergé, rond, turbulent et dirigé vers le haut frontalement à une surface libre. Des distributions de vitesse axiale sont présentées et comparées à celles correspondant à un jet libre. La distribution de vitesse radiale le long de la surface au-dessus du jet est mesurée et les résultats sont présentés en comparaison avec la distribution correspondant au cas d'un jet frappant une surface rigide. La configuration générale de l'écoulement dans le réservoir d'essai est observée par visualisation de l'écoulement.

On montre que la connaissance de ces paramètres est utile pour la modélisation du transfert de chaleur et de masse dans des écoulements de ce genre.

DAS GESCHWINDIGKEITSFELD EINES STRAHL, DER INNERHALB EINER FLÜSSIGKEIT SENKRECHT NACH OBEN GEGEN DIE FREIE OBERFLÄCHE GERICHTET IST

Zusammenfassung—In diesem Aufsatz wird die Strömung in einem runden turbulenten Wasserstrahl betrachtet, der senkrecht von unten gegen die freie Wasseroberfläche gerichtet ist. Die Verteilungen der Axial-Geschwindigkeit werden dargestellt und mit denen in einem entsprechenden Freistrahle verglichen. Die Verteilung der Radialgeschwindigkeit an der Oberfläche über dem Strahl wurde gemessen, die Ergebnisse dargestellt und mit der Verteilung in einem Wandstrahl, der auf eine feste Oberfläche auftrifft, verglichen. Die Strömungsformen im Versuchsbehälter wurden durch Sichtbarmachung der Strömung beobachtet. Es wird gezeigt, daß die Kenntnis dieser Parameter wertvoll für die Modellbildung von Wärme- und Stoffübertragungsvorgängen in Strömungen dieser Art ist.

ПОЛЕ СКОРОСТИ, СОЗДАВАЕМОЕ ЗАТОПЛЕННОЙ СТРУЕЙ, НАПРАВЛЕННОЙ ВВЕРХ К СВОБОДНОЙ ПОВЕРХНОСТИ ВОДЫ

Аннотация—Рассматривается течение круглой турбулентной затопленной струи воды, направленной вверх по нормали к свободной водной поверхности. Представлены осевые распределения скорости и проведено сравнение с соответствующими распределениями для свободной струи. Измерено радиальное распределение скорости на поверхности над струей и проведено сравнение полученных результатов с распределением скорости в поверхностной струе, возникающей при ударе о твердую стенку. Общий характер течения в экспериментальном резервуаре определялся с помощью визуализации потока. Показано, что указанные параметры необходимы для моделирования тепло-и массообмена в потоках такого типа.